Iron Losses in Ferromagnetic Enclosures of Gas-Insulated Transmission Lines under AC

W. WIEBEL[1]*, R.-D. ROGLER[1] AND J. KINDERSBERGER[2]

[1]University of Applied Sciences, Dresden, Germany

[2]Technical University of Munich, Munich, Germany

Abstract:

The enclosure of AC gas-insulated transmission lines (AC-GIL) is ordinarily made of aluminum. In HVDC systems, it can be economically and technically reasonable to manufacture the enclosure of GIL from steel. To check the feasibility to operate such DC-GIL even under AC the relevant losses in the steel enclosure must be known.

The present paper compares three different methods to determine the specific iron losses of steel when exposed to magnetic fields with power frequencies. The iron losses as a function of the magnetic field strength are measured with a pipe sample in a coaxial conductor arrangement, a pipe sample in a toroidal core test and with relevant strips in an Epstein frame. The results from the three test methods are found to be in good agreement. By calculating the iron losses in a GIL with steel enclosure the reduction of the transmission capacity is estimated when changing from DC to AC operation.

1. Introduction

The increasing use of renewable energy sources leads to longer distances between energy production and consumers. Onshore and offshore wind farms are examples for this trend. Transmission of high power over long distances is usually performed by means of HVDC transmission. The gas-insulated transmission lines (GIL) with steel enclosure represent one option for HVDC power transmission. For the sake of maximum flexibility in network operation, power transmission in relevant GIL sections should then also be possible by HVAC, provided that a third conductor is available. In order to calculate the transmission capacity of such GIL sections, the losses occurring under AC operation must be known.

For the determination of the specific iron losses and other material properties of electrical steel sheets and strips, which are usually used in rotating and stationary electrical machines as well as in electrical components, standardized measuring methods have been established. Among others, the determination can be carried out by means of Epstein frames [1], single-sheet tester [2], ring and parameter method [3]. In the standard measurement methods, steel sheets or strips are exposed to a magnetic field which is as homogeneous as possible. Thus, the samples experience a similar magnetic field situation like for example in static electrical machines.

In the vicinity of current-carrying conductors a concentric magnetic flux density is formed in accordance with Ampère's circuital law. Thus, the aforementioned standardized measuring methods cannot be adopted without checking their suitability. In the area of power cables, there are no standardized measurement methods for the direct determination of the losses in the enclosure caused by alternating magnetic field [4]. Power losses are determined in particular by calculation methods, e.g. IEC 600287-1 [5].

* wolfgang_wiebel@web.de

KEYWORDS

AC-losses, enclosure loss, GIL, iron losses, loss measurement

To verify the calculation models, the power dissipation in the enclosure can be determined by its temperature rise. The heat capacity of the enclosure, the temperature rise shortly after switching on the load current and the time at which the temperature change is recorded can be used to determine the power loss in the enclosure [6].

Alternatively, the losses of a conductor with and without shielding, conduit or pipe can be determined by measuring the current, the voltage and the phase shift. The losses in the metallic casing are the difference between the AC-losses with and without metallic casing. In most methods, the losses are given by the ratio of AC-Resistance to DC-Resistance of the test object [7] – [10]. Due to the lack of a relevant standard for the determination of the AC resistances, different measuring methods can be used [11].

Furthermore, in complex cable arrangements, e.g. in metallic cable ducts, the losses can be determined numerically after measuring the material parameters of the metallic casing. In [12] the material parameters of a cable duct were determined by Epstein frame. The calculated power losses correspond well to the measured values.

The experimental effort to determine the conduction losses in any kind of metallic casing is relatively high. To clarify whether the effort can be reduced by alternative experimental methods, three measuring methods for the determination of the specific losses were studied:

- High current test
- Ring core test
- Epstein frame

By using these methods, the specific losses of the steel grade L245 (acc. to ISO 3183), which is used notably in pipeline construction, are determined and represented as a function of the magnetic field strength [13].

With these methods, a statement can be made about the expected losses in metallic casings, e.g. enclosures of GIL or protective pipes of cables, by simple standardized tests.

2. Electromagnetic Basics

2.1. Quasistationary Electromagnetic Fields

The quasistationary electromagnetic fields can be described by a system of algebraic equations and partial differential equations. According to Ampère's circuital law, the current I corresponds to the line integral of the magnetic field strength H along the closed contour s around the conductor. The current can be also described by the current density S integrated over the area A [14]:

$$\oint_{(s)} \boldsymbol{H} \cdot \mathrm{d}\boldsymbol{s} = \iint_{(A)} \boldsymbol{S} \cdot \mathrm{d}\boldsymbol{A} = I \tag{1}$$

According to the law of induction, the induced voltage u_i corresponds to the magnetic flux density derivation $\mathrm{d}B \cdot \mathrm{d}t^{-1}$ over the area A. The line integral of the electric field strength $\boldsymbol{E}$ along the closed line s around this area results also in the induced voltage [14]:

$$u_\mathrm{i} = \oint_{(s)} \boldsymbol{E} \cdot \mathrm{d}\boldsymbol{s} = -\iint_{(A)} \frac{\mathrm{d}\boldsymbol{B}}{\mathrm{d}t} \cdot \mathrm{d}\boldsymbol{A} = -\frac{\mathrm{d}\phi}{\mathrm{d}t} \tag{2}$$

2.2. Magnetic Constant Field Measurement

The static hysteresis loop is measured using the magnetic constant field method. The iron losses, which in this case are identical to the hysteresis losses, are determined from the area of the hysteresis curve.

2.3. Magnetic Alternating Field Measurement

Further to the hysteresis losses, there are also eddy current losses and after-effect losses caused by diffusion processes in the metal texture, the latter type of loss being negligible [15]. These losses can be measured by exposing electrical sheets to 50 Hz magnetic fields.

Eddy Current Losses

According to the law of induction from (2), a voltage u_i is induced in the iron when the magnetic flux density $B(t)$ changes over time and the cross-section A_Fe remains constant.

$$u_\mathrm{i} = -A_\mathrm{Fe} \cdot \frac{\mathrm{d}B}{\mathrm{d}t} \tag{3}$$

Assuming a sinusoidal magnetic flux density we get:

$$u_\mathrm{i} = -A_\mathrm{Fe} \cdot \hat{B} \cdot \omega \cdot \cos(\omega t) = i_\mathrm{W}(t) \cdot R_\mathrm{Fe} \tag{4}$$

i_W is the time-dependent eddy current and R_Fe the equivalent ohmic resistance of the iron. The resistance depends on the geometry and the electrical conductivity of the object. $\hat{U}_i$ is the peak of the induced voltage of (4). The eddy current losses P_W result from:

$$P_{\mathrm{W}} = \frac{R_{\mathrm{Fe}} \cdot \hat{I}_{\mathrm{W}}^{\,2}}{2} = \frac{\hat{U}_{\mathrm{i}}^{\,2}}{2 \cdot R_{\mathrm{Fe}}} = \frac{\left(A_{\mathrm{Fe}} \cdot \hat{B} \cdot 2\pi \cdot f\right)^2}{2 \cdot R_{\mathrm{Fe}}} \tag{5}$$

$$\Longrightarrow \quad \boldsymbol{P_{\mathrm{W}} \sim B^2 \cdot f^2} \tag{6}$$

Hysteresis Losses

The hysteresis losses caused by friction of the *Weiss domains* can be determined from the area of the static hysteresis curve. According to [14] the losses are as follows:

$$P_{\mathrm{Hy}} = V_{\mathrm{Fe}} \cdot f \cdot A_{\mathrm{stat}} \tag{7}$$

V_{Fe} is the volume of the iron, f the frequency and A_{stat} the area of the static hysteresis curve.

Iron Losses (Remagnetization Losses)

The eddy current and hysteresis losses (as well as aftereffect losses) are summarized as iron losses or remagnetization losses.

$$P_{\mathrm{Fe}} = P_{\mathrm{W}} + P_{\mathrm{Hy}} \tag{8}$$

For characterizing a material the specific iron power loss p_{Fe} ($\mathrm{W \cdot kg^{-1}}$) has been introduced. For the user of electrical sheets, the specific losses depending on the magnetic flux density B are of particular interest. The functional relationship is described by a formula based on the *Steinmetz equation* [15]:

$$p_{\mathrm{Fe}} = \frac{P_{\mathrm{Fe}}}{m_{\mathrm{a}}} = k_{Hy} \cdot f \cdot B^n + k_W \cdot f^2 \cdot B^2 \tag{9}$$

m_{a} is the active mass of the sample. n, k_{Hy} and k_{W} are parameters which are determined from the measured power loss characteristics.

The magnetic flux density B is linked to the magnetic field strength H via the magnetic field constant μ_0 and the material-specific relative permeability μ_{r}.

$$B = \mu_0 \cdot \mu_r \cdot H \tag{10}$$

3. Test Object and Operating Conditions

3.1. Test Object and Material Sample

The test object is a pipe section with a height h_{r} of 102 mm and an inner diameter d_{i} of 161 mm (Fig. 1). The wall thickness l_{Wall} is 4 mm. The pipe section is made of the material L245 (acc. to ISO 3183). The mass of the sample is 1.590 kg.

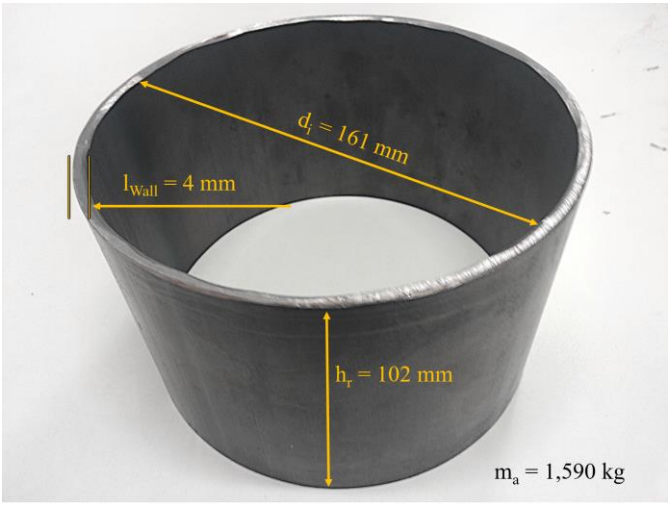

Fig. 1. Geometry and mass of the material sample L245 according to ISO 3183

3.2. Required Magnetic Field Strength

In practice, the current carrying capacity of GIL results from the total losses of the transmission line and the thermal boundary conditions (type of installation, permissible maximum temperatures, thermal conductivities, etc.).

Typical current ratings at 420 kV or 550 kV with an enclosure diameter of about 500 mm is between 3000 A and 4000 A. Typical current ratings and diameters of the enclosure for higher system voltages are summarized in Table 1 [16].

At rated current the resulting magnetic field strengths in the enclosure as per *Ampère's* circuital law (1) are also listed in Table 1.

TABLE I

TYPICAL CURRENT RATINGS AND DIAMETERS OF GIL

Variant	Current in A	Diameter in mm	Magnetic Field Strength in $\mathrm{A \cdot m^{-1}}$
420 kV or 550 kV	4000	500	2546
800 kV	5000	630	2526
1200 kV	6000	800	2387

Hence, for typical GIL designs and current ratings the magnetic field strength in the enclosure is in the range of 2500 $A \cdot m^{-1}$

3.3. Frequency

GIL are usually operated with direct current or with alternating current of 50 Hz or 60 Hz.

When determining the specific iron losses in the following tests, only the results measured at 50 Hz are presented.

Enclosure Temperature

The temperature limit of the enclosure depends on the type of installation.

If GIL or parts thereof can be touched, e.g. in tunnel or air-laid installations, the maximum permitted surface temperature is 70 °C. If the GIL is not exposed to get touched during normal operation, the temperature shall not exceed 80 °C [17].

From a technical point of view, the temperature limit of the encapsulation of directly buried GIL depends on the temperature resistance of the corrosion protection. With polypropylene coating the limit lies at 90 °C. In order to minimize, for example, the impact on soil flora and fauna caused by groundwater heating and soil dehydration, the temperature limit of the enclosure is usually subject to greater restrictions. Typical limit values are 40 °C or 50 °C [16].

3.4. Grounding

The enclosures of GIL are typically grounded at both ends. Therefore, under AC operation the induced voltage drives a current in the GIL enclosure which has almost the same magnitude but opposite polarity as the current in the inner conductor. In the experiments presented, only arrangements grounded on one side are considered.

4. Comparison of Measurement Methods

4.1. High Current Test

In the high current test, the mounting and magnetic excitation of the pipe section is like in a GIL.

Test Setup

The pipe sample is mounted concentrically around a copper conductor (Fig. 2). A high-current transformer feeds the current circuit. The current is measured using a *Rogowski coil*. The magnetic field strength in the steel enclosure can be determined with the *Ampère's* circuital law (1).

The voltage along the conductor is measured at two conductor sections:

- one at the pipe sample.
- the other one at an uninfluenced conductor section.

The voltage taps are equidistant and the measuring cables are crossed out to eliminate induced voltages.

The temperature is measured by thermocouples type K (acc. to IEC 60584-3) [18]. One is attached to the pipe sample and another one to the inner conductor. The power dissipation is determined when the pipe sample has reached the typical operating temperature of GIL-enclosures.

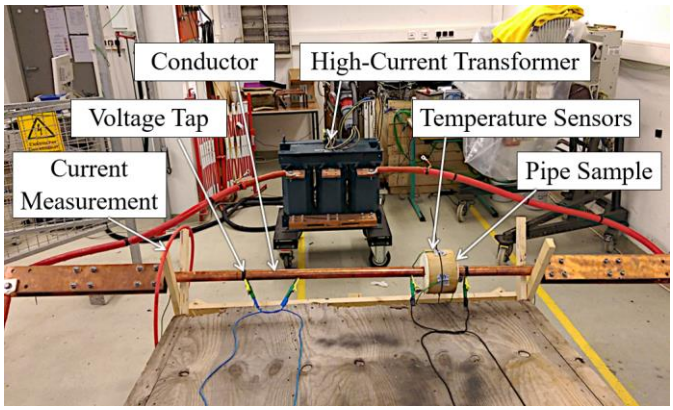

Fig. 2. High current test setup for the electrical determination of losses in steel enclosures

Loss Calculation

The power losses in the material sample could are determined by simply subtracting the total losses of the tube section from the losses of the conductor without tube.

The specific iron losses are the quotient of the power loss and the mass of the pipe sample (9).

Result of the High Current Test

In the test series currents of up to 1719 A were applied, which corresponds to a magnetic field strength of 3316 $A \cdot m^{-1}$. At the typical field strength of 2510 $A \cdot m^{-1}$ and an enclosure temperature of approx. 72.0 °C, the losses in the pipe section were 130 W which corresponds to specific losses of 81.5 $W \cdot kg^{-1}$.

The specific iron losses determined in the high current test as a function of the magnetic field strengths are shown in Fig. 7.

4.2. Ring Core Test

In accordance to IEC 60404-4, the hysteresis loop can be determined by means of a ring core test in a constant magnetic field. The area of the loop describes the hysteresis losses. However, no eddy current losses occur in the DC field, so the general conditions described in the standard were adopted and a different test procedure was chosen.

Test Setup

For the ring core test, the surface of the pipe sample is

insulated by insulating paper and tape. Then, the sample is wrapped with an enameled copper wire to form a toroidal coil with 438 windings around the pipe sample (Fig. 3).

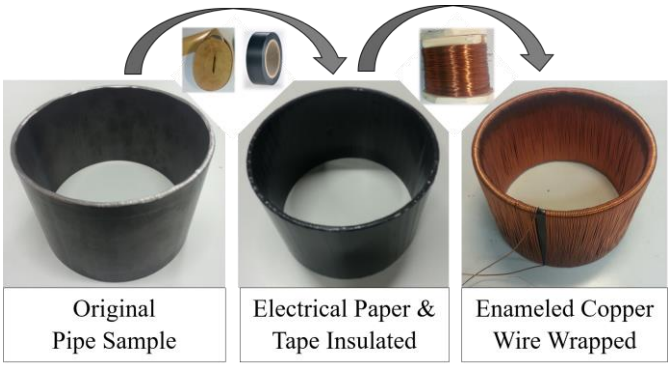

Fig. 3. Step-by-step procedure for preparing the pipe sample for the ring core test

With a variable voltage source it is possible to apply different currents at different frequencies to the coil (Fig. 4). According to the description in IEC 60404-4, the temperature of the material sample was kept below 50 °C by means of a fan [3].

A power meter is used to measure current, voltage, frequency and phase shift. The temperature of the pipe sample is measured by means of a thermocouple type K (acc. to IEC 60584-3) attached between insulating tape and electrical insulation paper.

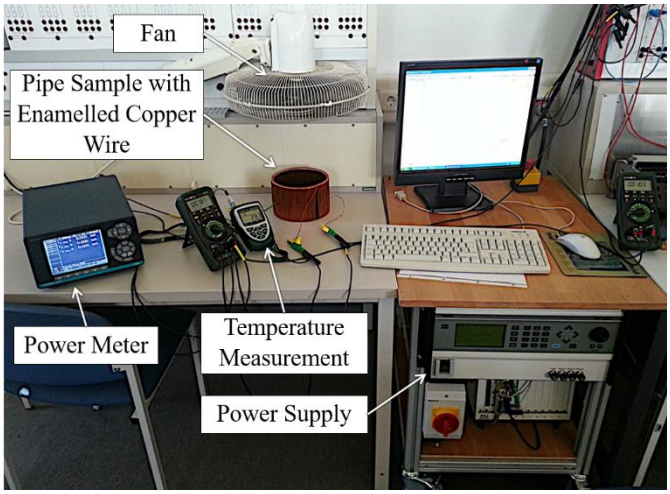

Fig. 4. Test setup of the ring core test for the determination of magnetic steel properties

Loss Calculation

The DC resistance of the copper wire was measured prior to the test. The iron losses are determined from the measured total losses minus the copper losses which are calculated from the temperature-corrected resistance of the copper wire.

Result of the Ring Core Test

The iron losses in the pipe sample were measured at magnetic field strengths up to 8500 $A \cdot m^{-1}$. At 2480 $A \cdot m^{-1}$, the losses in the pipe section were 118.2 W which corresponds to specific losses of 74.3 $W \cdot kg^{-1}$. This results in slightly lower losses compared to the high current test. One reason can be the temperature-correction of the wire. The temperature of the windings and the pipe sample is measured within the insulation. Depending on the losses, the winding experiences a natural or forced cooling. The temperature of the winding is probably slightly lower than measured. Thereby the copper losses are calculated slightly higher.

The specific iron losses of L245 in dependence of the magnetic field strength measured by the ring core method are shown in Fig. 7.

4.3. Epstein Frame

According to IEC 60404-2, *Epstein* frames are used to determine the magnetic properties of electrical steel strips and sheets [1]. However, the typical wall thicknesses of GIL enclosures are considerably greater than the cold rolled electrical steel sheets generally used in the electrical industry. Moreover, conventional steel has a higher electrical conductivity than electrical steel sheets.

In the *Epstein* frame four air coils are arranged in a square (Fig. 5). The magnetic field in each coil is almost homogeneous, and the strip-like samples to be measured are placed in the coils and connected at their ends to form a quadratic loop.

The mechanical processing and deformation required to measure the pipe sample in the *Epstein* frame might change the properties of the sheet metal.

Test Setup

In order to measure the tubular material sample in the *Epstein* frame, the pipe must first be sawn into pieces, straightened and cut into four equal sample strips. Each of the 4 mm thick strips has a length of 273 mm and a width of 23 mm. The strips of the sample material are inserted into the four air coils of the Epstein frame to form a square as shown in Fig. 5. According to IEC 60404-2, the total active mass of the four legs is 0.654 kg. The samples can be inserted, and the magnetic properties can be determined in accordance to IEC 60404-2.

The 25 cm *Epstein* frame consists of four coils. Each one of them is placed on a square coil former as a layer winding and connected in series. Each coil former carries two

windings, an outer primary winding to generate the magnetic field *H* for the excitation of the sample and an inner secondary winding to determine the magnetic flux density *B*. The coils are connected in series. Fig. 5 shows a section through the *Epstein* frame and the wiring of the coils.

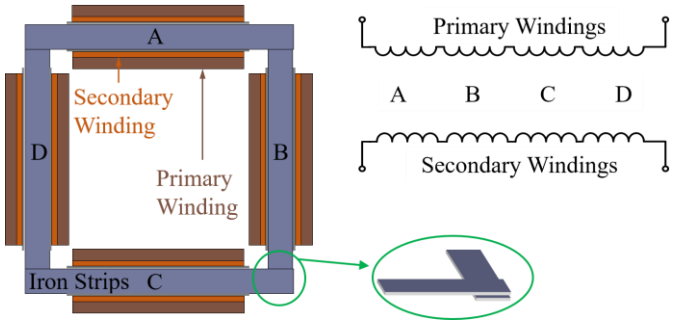

Fig. 5. Section through the 25 cm *Epstein* frame with sample material (left) and wiring of the coils on the primary and secondary side (right).

The primary windings of the *Epstein* frame are energised by a variable voltage source. The consumed power is measured by a power meter. The cold resistance of the primary winding is measured before the test (Fig. 6).

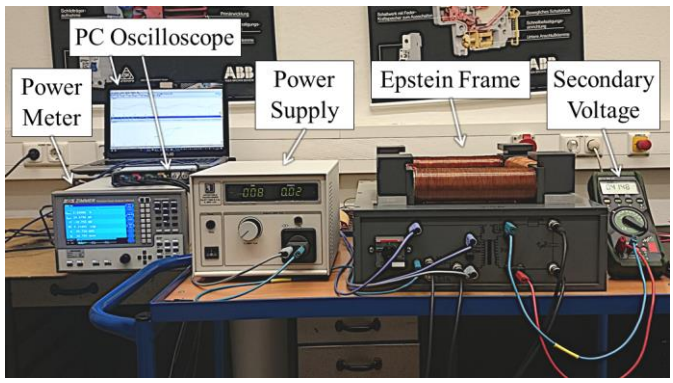

Fig. 6. Test setup of the 25-cm-*Epstein* frame for measuring the magnetic properties of the steel

Loss Calculation

In order to determinate the iron losses, the total power consumption in the *Epstein* frame needs to be measured. The iron losses of the sample are calculated by subtracting the copper losses of the primary windings from the total power consumption.

Result of the Epstein Frame

In order to allow a comparison with the previous measurements, the temperature of the sample was set to 72.0 °C. At this temperature and at a magnetic field strength of 2680 A·m^{-1} the losses in the sample strip arrangement were 52.6 W which corresponds to specific power loss of 80.5 W·kg^{-1}. The specific losses determined in the *Epstein* frame are shown in Fig. 7.

Thus, the measured specific losses correspond well to the values measured in the ring core test and in the high-current test. In the measured steel sample L245, there were no significantly higher losses, e.g. due to the influence of the additional cutting edges of the samples. The slight deviation may be caused by the air gap at the corners of the *Epstein* frame.

The test shows that material samples for the production of enclosure materials can also be measured using the standardized *Epstein* frame method.

5. Summary of the Results

5.1. Evaluation of the Results

The investigation shows that all three methods are suitable to determine the iron losses in material samples of GIL enclosures. The three different measurement methods lead to similar iron losses for magnetic field strengths up to 3000 A·m^{-1}. Fig. 7 shows the specific power loss of the 4 mm steel sheet L245 measured with the high-current test, ring core test and *Epstein* frame as a function of the magnetic field strength.

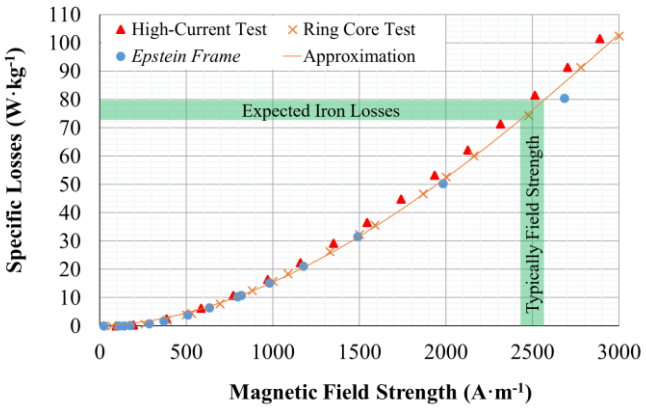

Fig. 7. Specific iron losses of L245 according to ISO 3183 in dependence of the magnetic field strength up to 3000 A·m^{-1} at a frequency of 50 Hz determined by high current test, ring core test and *Epstein* frame.

From the results of the measurement the specific losses depending on the magnetic field strength can be approximated by (11).

$$p_{\mathrm{Fe}} = \frac{P_{\mathrm{Fe}}}{m_{\mathrm{a}}} = k_1 \cdot H + k_2 \cdot H^2 + k_3 \cdot H^3 \qquad (11)$$

The material sample of L245 for the steel enclosure can

be characterized by the following coefficients for $H < 3000$ A m^{-1}:

$$k_1 = 2.3 \cdot 10^{-3} \frac{V \cdot m}{kg} \quad (12)$$

$$k_2 = 1.4 \cdot 10^{-5} \frac{V \cdot m^2}{A \cdot kg} \quad (13)$$

$$k_3 = -1.2 \cdot 10^{-9} \frac{V \cdot m^3}{A^2 \cdot kg} \quad (14)$$

5.2. Impact on GIL

In AC operation, the magnetic flux density caused by the current in the inner conductor, induces a voltage causing a current in the GIL enclosure which has almost the same magnitude but opposite polarity as the current in the inner conductor, provided the enclosure of GIL is grounded at both ends. The total losses of AC GIL are mainly caused by the current in the inner conductor and in the enclosure. Typical losses of AC GIL with aluminum conductor and aluminum enclosure are in the range of 120 W·m^{-1} (in 420-kV-GIL) to 240 W·m^{-1} in 1200-kV-GIL [16]. At a constant resistivity, the losses are in direct proportion to the current in square (5).

The mass density of the material sample can be calculated from its dimensions and mass (Fig. 1). Using the diameters, listed in Table 1, and the wall thickness of the material sample, a length related mass of 47.2 kg·m^{-1} (at 420 kV GIL) to 94.5 kg·m^{-1} (at 1200 kV GIL) is obtained.

Given that a DC-GIL with ferromagnetic enclosure shall be operated under AC, the total losses of the AC operation shall not exceed the losses under DC operation in order not to exceed the maximum permissible temperature. When using an enclosure made of L245 with one-sided grounding, the iron losses dominate even the resistance of the inner conductor increases due to the skin effect. Assuming an equal resistance of the inner Conductor, the magnetic field strength for the same loss density like in AC GIL can be calculated by (11) and (5). For example, in a 420 kV GIL with a 4 mm thick enclosure made of steel grade L245, the maximum AC current loading could be only about 9.1 % compared to the nominal DC current. In that case, iron losses in the enclosure dominate with 119.0 W compared to 1.0 W current heat losses in the inner conductor.

6. Conclusion

In view of the lack of a standardized method to determine the iron losses in the steel encapsulation of a gas insulated transmission line (GIL) under AC operation three different methods to determine the iron losses in steel samples are studied. It is shown that the iron losses for steel grade L245 measured with a pipe sample in a coaxial conductor arrangement, a pipe sample in a toroidal core test and with relevant strips in an Epstein frame leads to well matching results.

In principle, DC-GIL can be operated also under AC. However, due to the relatively high iron losses in DC-GIL with encapsulations made for example from L245 the permissible AC current loading is significantly reduced compared to the nominal DC current loading. This effect can be decreased by using steel grades with low specific losses.

7. Acknowledgment

This work was supported by the Federal Ministry for Economic Affairs and Energy (FKZ: 03ET7511C).

8. References

[1] Magnetic materials - Part 2: Methods of measurement of the magnetic properties of electrical steel strip and sheet by means of an *Epstein* frame, IEC 60404-2, 1996

[2] Magnetic Materials – Part 3: Methods of measurement of the magnetic properties of magnetic sheet and strip by means of a single sheet tester, IEC 60404-3, 1992

[3] Magnetic materials – Part 4: Methods of measurement of d.c. magnetic properties of magnetically soft materials, IEC 60404-4, 1995

[4] Large cross-sections and composite screens design, Cigré Working Group B1.03. 272, CIGRE, 2005

[5] Electric cables - Calculation of the current rating - Part 1-1: Current rating equations (100 % load factor) and calculation of losses IEC 60287-1-1:2006/AMD1:2014

[6] K. Kawasaki, M. Inami and T. Ishikawa, "Theoretical Considerations on Eddy Current Losses in Non-Magnetic And Magnetic Pipes for Power Transmission Systems," IEEE Transactions on Power Apparatus and Systems, vol. PAS-100, Issue: 2, Feb. 1981, pp. 474-484

[7] R. W. Burrell and M. Morris, "A-C Resistance of Conventional Strand Power Cables in Nonmetallic Duct and in Iron Conduit," IEEE Transactions of the American Institute of Electrical Engineers Part III: Power Apparatus and Systems, vol. 74, Issue: 3, Jan. 1955, pp. 1014-1023

[8] AIEE Committee Report, "A-C Resistance of Pipe-Cable Systems With Segmental Conductors," IEEE Transactions of the American Institute of Electrical Engineers Part III: Power Apparatus and Systems, vol. 71, Issue: 1, Jan. 1952, pp. 393-414

[9] R. J. Wiseman, "A-C Resistance of Large Size Conductors in Steel Pipe or Conduit," IEEE Transactions of the American Institute of Electrical Engineers, vol. 67, Issue: 2, Jan. 1948, pp. 1745–1758

[10] L. Meyerhoff and G. S. Eager, "A-C Resistance of Segmental Cables in Steel Pipe," IEEE Transactions of the American Institute of Electrical Engineers, vol. 68, Issue: 2, July 1949, pp. 816-834

[11] R. Suchantke, „Alternating current loss measurement of power cable conductors with large cross sections using electrical methods,“ Ph.D. dissertation, Inst. Energie- und Automatisierungstechnik, TU Berlin, Germany, 2018

[12] P. Sergeant and S. Koroglu, „Electromagnetic losses in magnetic shields for buried high voltage cables,“ Progress in Electromagnetics Research B, vol. 115, pp. 441-460, Jan. 2011

[13] W. Tirler, “Stahlsortenvergleich mit chemischer Analyse,” in International Comparison of Steels, 2nd ed. Berlin, Wien, Zürich, Germany, Austria, Switzerland: Beuth Verlag GmbH, 2016, p. 1204

[14] K. Küpfmüller, W. Mathis and A. Reibiger, *Theoretische Elektrotechnik - Eine Einführung*. 19th ed. Berlin Heidelberg, Germany: Springer-Verlag, 2013, pp. 301–465.

[15] S. Flohrer, “Analyse der dynamischen Magnetisierungsprozesse nanokristalliner Weichmagnete,” Ph.D. dissertation, Inst. F. Werkstoffwissenschaft, Fak. Maschinenwesen, TU Dresden, Germany, 2007

[16] H. Koch, “Current Rating,” in Gas-Insulated Transmission Lines (GIL), 1st ed. Chichester, West Sussex, PO19 8SQ, United Kingdom, John Wiley & Sons Ltd., 2012, pp. 328-329

[17] High-voltage switchgear and controlgear - Part 1: Common specifications for alternating current switchgear and controlgear, IEC 62271-1, 2017

[18] Thermocouples – Part 3: Extension and compensating cables – Tolerances and identification system, IEC 60584-3, 2007

[19] G.M. Harvey and A.H.W. Busby, “The use of single-core armoured cables for alternating currents,” IEEE Journal of the Institution of Electrical Engineers, vol. 63, Issue: 340, April 1925, pp. 368-378

Wolfgang Wiebel. He received the Dipl.-Ing. (FH) and the M.Sc. degrees from the University of applied Sciences Dresden (HTW Dresden) in 2012 and 2013, respectively.

From 2012 to 2017, he was with the Centre of Applied Research and Technology at Dresden University of Applied Sciences. Since 2017 he is with the R&D-Department and Test Field of the Starkstrom-Gerätebau GmbH in Regensburg.

Wolfgang Wiebel is member of VDE.

Ralf-Dieter Rogler received the Dipl.-Ing. and the Dr.-Ing. degrees from the Technical University of Dresden (TUD) in 1994 and 1999, respectively.

In 1998 he has founded Theta Ingenieurbüro, which among other things dealing with diagnosis, evaluation and further development of electrotechnical devices and systems. In 2005 he was appointed to the University of Applied Sciences for Switchgear Technology.

He is active in VDE AK 2 (high-voltage equipment and systems).

Josef Kindersberger (M’87). He received the Dipl.-Ing. and the Dr.-Ing. degrees from the Technical University of Munich (TUM) in 1979 and 1986, respectively. From 1986 to 1995 he was with the High Voltage Insulator Group of Hoechst CeramTec AG in Wunsiedel. In 1995 he became full professor at the Technical University of Dresden. From 2001 until 2019 he was head of the Chair of High Voltage Engineering and Switchgear Technology at the Department of Electrical and Computer Engineering of the Technical University of Munich (TUM), Germany.

He is active in CIGRE (Chairman of SC D1, 2010-2016), IEC (Chairman of TC 36, 2003-2015), IEEE and VDE/ETG.